Available online at www.sciencedirect.com
ScienceDirect
Applied Surface Science 253 (2006) 1666–1672
applied surface science
www.elsevier.com/locate/apsusc

Superior thermal stability of Ta/TaN bi-layer structure for copper metallization

Qi Xie, Xin-Ping Qu *, Jing-Jing Tan, Yu-Long Jiang, Mi Zhou, Tao Chen, Guo-Ping Ru

Fudan-Novellus Interconnect Research Center, Department of Microelectronics, Fudan University, Shanghai 200433, China

Received 19 December 2005; received in revised form 12 February 2006; accepted 1 March 2006
Available online 30 June 2006

Abstract

Ta/TaN bi-layer structure is currently used in the ultra-large scale integrated circuits (ULSI) interconnect as barrier for copper because of its good adhesion to both SiO_2 and Cu wire. In this work Cu, Ta and TaN layers were prepared by sputtering technology. X-ray diffraction, Auger electron spectroscopy (AES), X-ray photoelectron spectroscopy (XPS) as well as transmission electron microscopy (TEM) were applied to characterize the thin film thermal stability and microstructure evolution. The results show that the Ta/TaN bi-layer structure has much better diffusion barrier properties than pure Ta or pure TaN film. A mechanism was proposed to explain the better thermal stability of the Ta/TaN bi-layer structure based on the correlation between TaN layer thickness and TaN crystallization kinetics. The microstructure evolution for Ta/TaN bi-layer structure during annealing was described.

PACS: 85.40.Ls; 66.30.Ny; 6630.Xj

Keywords: Copper interconnect; Diffusion barrier; Thermal stability; Ta/TaN

1. Introduction

Tantalum (Ta) and tantalum nitride (TaN) barrier layers have been extensively used in Cu interconnection system due to their good diffusion barrier properties and relatively stable structure [1–19]. Ta and TaN as diffusion barriers have been individually investigated comprehensively [1–12]. Ta has better adhesion with Cu [4,5] and acts as a nucleation layer for Cu [13]. TaN is a good diffusion barrier due to its amorphous or nano-crystalline characteristics [14]. A lot of efforts have been taken to improve the barriers performance. Ou et al. showed that intentionally forming an amorphous layer on the surface of TaN by plasma treatment would improve barrier layer properties of TaN against Cu diffusion [9]. Epitaxial growth of a cubic phase TaN on Si using a TiN buffer layer was reported by Wang et al. [15]. Chen et al. revealed that adequately designed Ta_2N/TaN multilayered films would block the Cu penetration more efficiently [16]. In industry, the Ta/TaN bi-layer structure configuration is used in which Ta is the adhesion layer between the Cu and TaN is the adhesion layer to the dielectrics. It is said that the advantage by using this configuration is that, the barriers would adhere well to both dielectric and Cu. In this work, the advantages of this bi-layer configuration other than its good adhesion to both SiO_2 and Cu wire have been investigated. The Ta/TaN bi-layer structure shows better thermal performance than pure Ta or pure TaN diffusion barriers. The reason for the better thermal stability of the Ta/TaN bi-layer structure was explained. Microstructure evolution for the Ta/TaN bi-layer structure during thermal annealing was discussed in details. This work gives an indication on how to reduce the barrier thickness in the future 65 nm technology node or beyond from the material's aspect.

2. Experiments

Two hundred millimeter diameter n-type Si(1 0 0) wafers were used as the starting substrates. A 700 nm SiO_2 thin film

* Corresponding author. Tel.: +86 21 65643561; fax: +86 21 65643768.
E-mail address: xpqu@fudan.edu.cn (X.-P. Qu).

0169-4332/$ – see front matter © 2006 Elsevier B.V. All rights reserved.
doi:10.1016/j.apsusc.2006.03.002

was deposited using NOVELLUS Concept One 200 plasma enhanced chemical vapor deposition (PECVD) system. The deposition temperature was 400 °C. The Ta-based barriers including Ta, TaN and Ta/ TaN bi-layer were deposited on both Si and SiO_2/Si wafers by INOVA Concept Two sputtering system. The Ta target is hollow cathode magnetron (HCM) target. Before PVD of metal layers the SiO_2/Si wafers were sent to Damaclean module to pre-clean the sample surface. The base pressure of PVD chamber was 5×10^{-8} Torr and the working pressure was about 5×10^{-5} Torr. The sputtering power was about 18 kW. TaN was reactively sputtered by flowing N_2 into Ar with a ratio of Ar: N_2 at 108 to 15 sccm. Cu seed layer was deposited sequentially without breaking the vacuum. After film deposition, the wafers were cut into small pieces and annealed by rapid thermal annealing (RTA) in high purity N_2 ambient at temperature range from 300 to 985 °C. The annealing duration was 1 min unless otherwise stated. Sheet resistance measurements were employed using a four-point probe. The phase formation for the as-deposited and annealed films was investigated by X-ray diffraction (XRD). Depth profiling Auger electron spectroscopy (AES) was used to investigate the atomic redistribution annealing. X-ray photoelectron spectroscopy (XPS) was used to measure the composition for copper surface. The microstructure for Cu/Ta/TaN bi-layer structure after annealing was characterized by cross-sectional transmission electron microscopy (XTEM).

3. Results

3.1. Thermal stability comparison among the Ta, TaN and Ta/TaN barriers

The thermal stability of the Ta, TaN and Ta/TaN structures on the Si substrates as the diffusion barriers for copper is compared. The total thickness of each kind barrier is fixed at 30 nm, while in the Ta/TaN bi-layer structure the Ta layer was 20 nm and the TaN layer was 10 nm. The thickness of the Cu film was 150 nm. Fig. 1 shows sheet resistance variation for the Cu/Ta/Si, Cu/TaN/Si and Cu/Ta/TaN Si samples as a function of annealing temperatures. It can be seen that the sheet resistance of the Cu/TaN/Si structure increases rapidly when the annealing temperature is higher than 700 °C; while the sheet resistance for the Cu/Ta/Si structure sharply increases upon annealing at 775 °C. The Ta/TaN bi-layer structure shows the best thermal stability, with increased sheet resistance only upon annealing temperature of 900 °C. We also annealed the three kinds of samples at 600 °C for 30 min among which the Ta/TaN structure also has the best thermal stability.

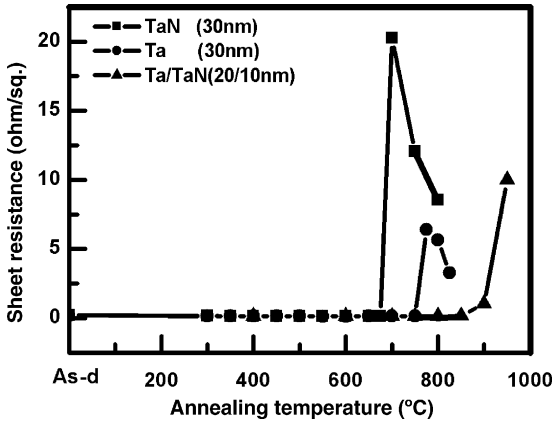

Fig. 1. The sheet resistance variations as a function of the annealing temperatures for the Cu/Ta, Cu/TaN and Cu/TaN/Ta layers on the Si substrate, respectively.

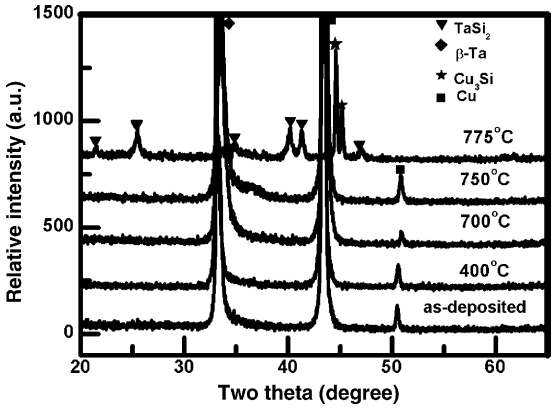

Fig. 2. XRD spectra of the Cu(150 nm)/Ta(30 nm)/Si samples annealed at different temperatures.

To further investigate the phase variation during annealing, XRD is carried out for the Cu/Ta/Si, Cu/TaN/Si and Cu/Ta/TaN/Si samples annealed at different temperatures. Fig. 2 shows the XRD spectra of the Cu(150 nm)/Ta(30 nm)/Si samples annealed at different temperatures. In the as-deposited sample, only β-Ta and Cu peaks can be observed. It should be mentioned that the XRD peak with d value of 2.67 Å ($2\theta = 33.28°$) should be indexed as β-Ta while not Si substrate peak since the half width of this peak is much larger than the normal Si substrate peak (please compare with Fig. 3). Only β-Ta and Cu peaks are detected in the samples annealed at temperatures lower than 750 °C. After annealing at 775 °C, $TaSi_2$ and Cu_3Si peaks are observed. The formation of the high resistive $TaSi_2$ and Cu_3Si phases would cause sharp increase of

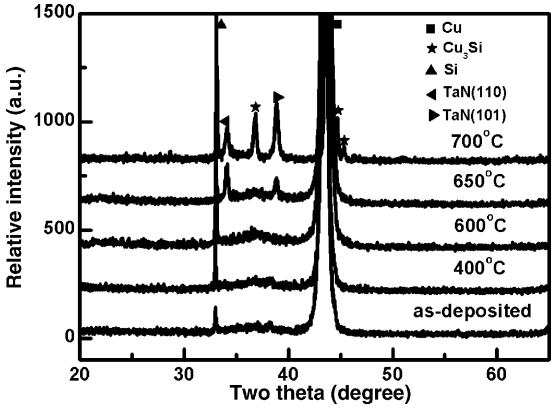

Fig. 3. XRD spectra of the Cu(150 nm)/TaN(30 nm)/Si samples annealed at different temperatures.

the sheet resistance of the Cu/Ta/Si structure after 775 °C annealing (shown in Fig. 1) and indicates the failure of the diffusion barrier.

Fig. 3 gives the XRD spectra of the Cu(150 nm)/TaN(30 nm)/Si structure annealed at different temperatures. For the samples annealed at temperatures lower than 600 °C, only Cu(1 1 1) peak appears. No TaN peaks can be observed, which demonstrates the amorphous structure of the as-deposited TaN film. After annealing at 650 °C, two new peaks which can be indexed as TaN(1 1 0) and TaN(1 0 1) appear, demonstrating the crystallization of the 30 nm TaN film upon annealing at 650 °C. After annealing at 700 °C the TaN peak intensity increases. The appearance of the Cu_3Si peaks demonstrates the failure of the barrier. The increased intensity of the TaN XRD peak indicates the crystallization and grain growth for the TaN phase. It has been assumed that the transition from amorphous structure to polycrystalline structure for the TaN will cause its failure as the diffusion barrier to copper [20]. The grain boundaries of the polycrystalline TaN layer would provide paths for fast Cu diffusion to the Si substrate and cause the formation of Cu_3Si.

The XRD spectra of the Cu(150 nm)/Ta(20 nm)/TaN(10 nm)/SiO_2/Si and Cu(150 nm)/Ta(20 nm)/TaN(10 nm)/Si samples annealed at different temperatures are given in Fig. 4(a) and (b), respectively. In both Fig. 4(a) and (b), we can see that no TaN peaks can be observed for the samples annealed at 400 °C. Different to Fig. 2, α-Ta peak appears. It has been reported that when growing on the TaN surface, the deposited Ta is α-Ta phase, whose resistivity is lower than that of the β-Ta, which is considered as one of the advantages for the Ta/TaN bi-layer configuration [21]. For samples annealed from 400 to 700 °C, what is interesting for these two figures is that there exits a transition region for peaks with 2θ from 38.2° ($d = 2.354$ Å) to 34.5° ($d = 2.6$ Å). The peak at $2\theta = 38.2°$ is indexed as α-Ta(1 1 0), while the peak at $2\theta = 34.5°$ is indexed as TaN(1 1 0). This XRD peak transition indicates the structural change for the original Ta/TaN bi-layer after annealing, which we will further investigate using AES and TEM. Both samples show superior thermal stability. The $TaSi_2$ and Cu_3Si peaks are observed only after annealing at 950 °C for the Cu/Ta/TaN/Si samples. On the SiO_2 substrate, after annealing at 985 °C, although copper peak is still the major peak, lots of ternary oxide $CuTa_{10}O_{26}$ peaks appear. It should be noted that for both the Cu/Ta/TaN/Si and Cu/Ta/TaN/SiO_2/Si samples, there appears one TaN XRD peak after annealing at 700 °C, which is 50 °C higher than the crystallization temperature (650 °C) for 30 nm TaN single-layer capped by Cu (as shown in Fig. 3). This indicates that the thickness of TaN layer may play a role on the crystallization temperature of TaN also, which would be investigated in the later part.

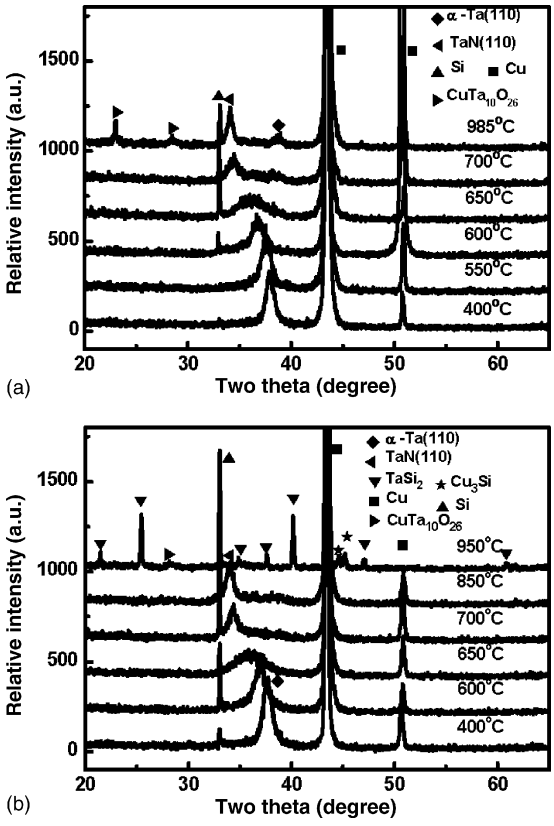

Fig. 4. (a) XRD spectra of the Cu(150 nm)/Ta(20 nm)/TaN(10 nm)/SiO_2/Si samples annealed at different temperatures and (b) the Cu(150 nm)/Ta(20 nm)/TaN(10 nm)/Si samples annealed at different temperatures.

3.2. Microstructure evolution for the Cu/Ta/TaN on SiO_2 and Si substrate

The XTEM images for a Cu/Ta/TaN/SiO_2/Si sample annealed at 750 °C are shown in Fig. 5. The low magnification images show that the interfaces for both Cu/Ta and TaN/SiO_2 are rather smooth (not shown here). As seen in Fig. 5(a), there is a 3 nm thick amorphous layer between the polycrystalline Cu and Ta layers. The amorphous layer was also observed by Kwon et al. and was believed to be caused by solid-state amorphization between Cu and Ta [4,5]. Yin et al. pointed out that the amorphous layer was caused by the penetration of the oxygen through the copper layer to the Ta layer and oxidation of the Ta layer; thus the amorphous layer was Ta-oxide layer and its thickness would increase after further annealing [22]. However, in this work we did not observe thickness increase of this amorphous layer after annealing. Whether the layer is oxide or not, it undoubtedly increases the thermal stability of the Cu/Ta/Si and Cu/Ta/TaN/Si structures. The Cu grains are very large. The selected area diffraction (SAD) pattern shown in the inset of Fig. 5(a) presents a single crystalline diffraction pattern of the copper. Although the interface between the Ta and TaN layers is not very flat, the Ta and TaN layers can be distinguished by the different contrast (Fig. 5(b)). As can be seen from Fig. 5(c), some TaN crystallites are surrounded by amorphous TaN, which indicates that the TaN layer was locally crystallized. However, the micro-diffraction pattern in the inset of Fig. 5(c) demonstrates that the whole TaN film is basically amorphous.

Since Cu is easier to react with Si than SiO_2, to further characterize the thermal stability of the Ta/TaN bi-layer structure, a Cu(150 nm)/Ta(20 nm)/TaN(10 nm)/Si sample was annealed at 800 °C for 1 min. The XTEM image of this sample

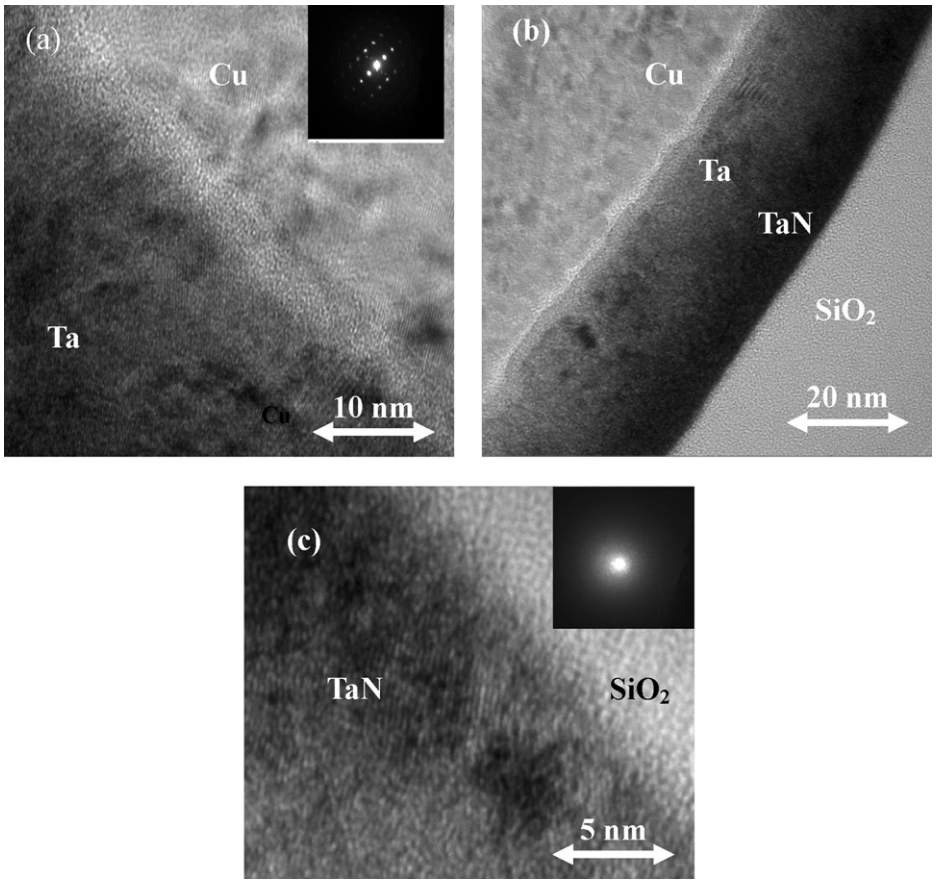

Fig. 5. XTEM images for a Cu(150 nm)/Ta(20 nm)/TaN(10 nm)/SiO_2/Si sample annealed at 750 °C for 60 s. (a) Top Cu/Ta layer. The inset shows the microdiffraction pattern for the Cu layer. Notice there is an amorphous layer between Cu and Ta films; (b) Ta/TaN bi-layer; (c) interface of barrier and SiO_2, the inset shows the microdiffraction pattern of the TaN layer.

in Fig. 6 shows that there is no obvious Cu reaction with Si substrate, which demonstrates superior thermal stability of the Ta/TaN bi-layer. EDS is used to detect the Cu concentration and three points labeled as 1, 2 and 3 are taken from the upper, middle and lower part of the Ta/TaN bi-layer, respectively. The EDS results show that, the Cu concentration for point 1 and point 2 is 7.6% and 1.23%, respectively. No Cu can be detected by EDS for point 3.

From Fig. 6 we can also see that the Ta and TaN layers become more mixed and are difficult to be differentiated compared with Fig. 5. Also as shown in Fig. 4, there is a transition region from Ta to TaN in the XRD spectra with increasing annealing temperature. This transition relates to the structural and compositional change for the bi-layer structure. AES depth profiles of the as-deposited Cu/Ta/TaN/SiO_2/Si sample and the one annealed at 800 °C are compared, shown in Fig. 7(a) and (b). Although the AES instrument resolution is not good, we can still see from Fig. 7(a) that the barrier is composed of one Ta-rich layer and one TaN_x layer. After annealing at 800 °C, Fig. 7(b) shows that the Cu layer keeps almost intact and the original Ta and TaN bi-layer become a mixed layer with N diffusing into the Ta layer. The whole layer is a Ta-rich TaN_x layer. So the XRD results in

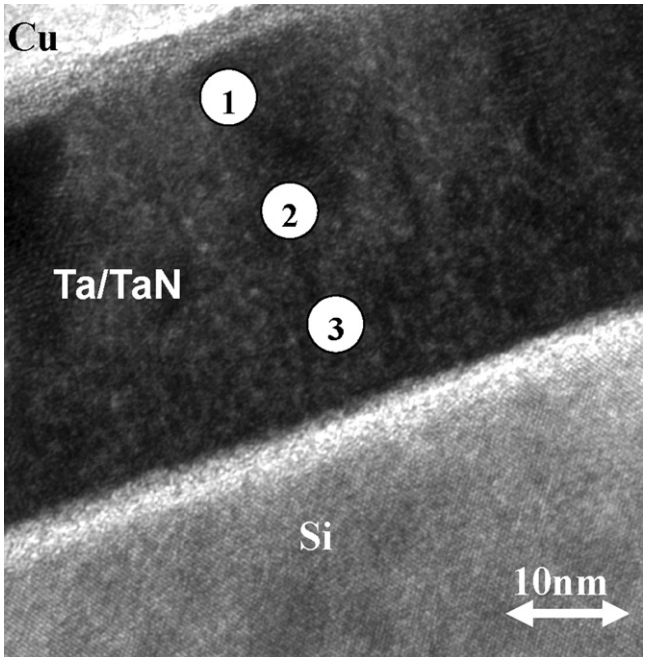

Fig. 6. XTEM image of a Cu(150 nm)/Ta(20 nm)/TaN(10 nm)/Si sample annealed at 800 °C.

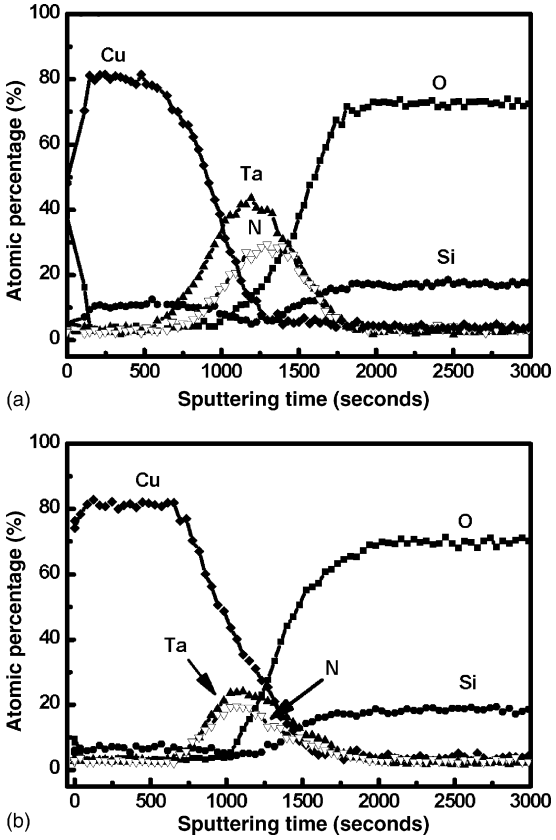

Fig. 7. (a) AES depth profiles of an as-deposited Cu(150 nm)/Ta(20 nm)/TaN(10 nm)/SiO_2/Si sample; (b) AES depth profiles of a Cu(150 nm)/Ta(20 nm)/TaN(10 nm)/SiO_2/Si sample annealed at 800 °C.

Fig. 4 can be explained as follows: the as-deposited Ta layer has a corresponding XRD peak. The as-deposited TaN was amorphous without appearance of XRD peak. With increasing annealing temperature, the N diffuses from the TaN to the Ta layer and Ta would incorporate with N to form TaN_x, whose lattice parameter is larger than that of Ta. After annealing at higher temperature, the TaN layer crystallizes with appearance of the TaN diffraction. The mixing of the bi-layer can be further confirmed by comparing Figs. 5 and 6.

During annealing, not only the original TaN and Ta layer intermixes, but also Ta outdiffuses through the copper layer to the copper surface. XPS technique is employed to detect the surface composition of the samples after annealing. Cu, O, C and Ta signals are detected in the full spectrum XPS and their concentrations are around 66%, 21%, 12% and 1%, respectively. Fig. 8 gives a high resolution XPS spectra of Ta 4f core level for a Cu(150 nm)/Ta(20 nm)/TaN(10 nm)/SiO_2/Si sample annealed at 750 °C. Ta $4f_{5/2}$ and $4f_{7/2}$ peaks from suboxide TaO_x and Ta_2O_5 are all observed in the high resolution XPS spectra, seen in Fig. 8. The binging energy of Ta $4f_{7/2}$ from suboxide TaO_x is 22.6 eV [23]; while that from Ta_2O_5 is 26.8 eV. Thus, Ta is believed to outdiffuse to the Cu surface alongside Cu grain boundaries and is oxidized. It should be noted that for samples annealed at 750 °C, no Si signal is detected by XPS, which indicates no Si outdiffusion at this temperature.

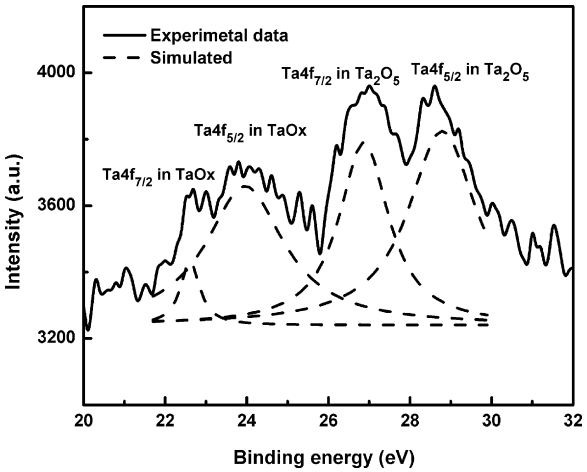

Fig. 8. XPS spectrum of Ta 4f core level for a Cu(150 nm)/Ta(20 nm)/TaN(10 nm)/SiO_2/Si sample surface annealed at 750 °C.

4. Discussion

The XRD results shown in Figs. 3 and 4 demonstrate that with the Cu capping layer, the TaN crystallization temperature for the Ta(20 nm)/TaN(10 nm) bi-layer structure is 50 °C higher than that for TaN(30 nm) single-layer. This indicates that TaN crystallization temperature may have size dependence, namely, the thickness of TaN layer will affect its crystallization.

As well known, the crystallization energy barrier ΔG^* for a crystallite is related to $\sigma^3/\Delta G^2$, where σ is the surface and interface energy change, and ΔG is the free energy change for a system [24,25]. Generally, the crystallite will take the form of either sphere or column, depending on the film thickness. Since sphere has smaller surface area than column for the same volume, the surface energy increase should be lower if the film starts crystallization from sphere rather than column. Thus, the nucleation energy barrier for sphere crystallization is lower than column crystallization, which causes the lower crystallization temperature for sphere crystallization. When the film is thick enough, the crystallite will take sphere shape due to its less surface area and a lower free energy for the system. The as-deposited TaN layer is amorphous. During annealing, TaN will crystallize. If the TaN layer is too thin to form sphere crystallite, it has to change to columnar crystallization due to the limit of vertical dimensions. The columnar TaN grain was observed by Lee et al. [7]. However, with the same volume for columnar crystallization, the surface-to-volume ratio is larger if the ratio of h-to-r is smaller (h is height, namely the film thickness and r is the radius of the column, respectively). The crystallization energy barrier increases with decreasing film thickness (h-to-r ratio decreasing) because the surface-to-volume ratio of the crystallite increases (more positive surface energy), which was also observed by Ma et al. for the Ti disilicide transition from C_{49}-to-C_{54} [26,27]. The increased crystallization temperature with decreasing of film thickness was confirmed by our experiment. A Cu/TaN/SiO_2 sample with TaN thickness of 8 nm was prepared and annealing at different temperatures was carried out. The XRD results (not shown here) showed that no

TaN peak could be detected at annealing temperatures lower than at 850 °C. However, the TaN peaks can be detected by XRD for the Cu(150 nm)/TaN(30 nm)/Si sample annealed at 650 °C (seen in Fig. 3).

Hereby it demonstrates that there would be a trade-off for the thickness of TaN diffusion barrier. To block the diffusion of Cu into dielectrics the TaN layer should be thick enough. Given the Cu diffusion length is proportional to $(Dt)^{1/2}$ (D is diffusion coefficient and t is diffusion time), the ideal case is that the barrier thickness should be larger than the Cu diffusion length. However, the TaN layer could not be too thick due to the decreasing of crystallization temperature with increasing of the thickness. Thus, one of the advantages of Ta/TaN bi-layer diffusion barrier is attributed to the fact that the bi-layer structure provides thick enough barrier (with the additional Ta layer) while TaN layer itself is still thin to have a high crystallization temperature.

Another important feature is that, for the Cu/TaN(30 nm)/Si and Cu/Ta(30 nm)/Si samples, the Cu_3Si phase formed after annealing at 700 and 775 °C, respectively; but for the Cu/Ta(20 nm)/TaN(10 nm)/Si sample, no Cu_3Si was observed until annealing at 950 °C. This result is quite surprising. We believe it should be attributed to the barrier layer microstructure. Although XRD results show that both Ta and TaN crystallize after annealing at 700 °C (Fig. 4), TEM results show that the TaN is only locally crystallized (Fig. 5(c)). Cu atoms would first diffuse along the Ta grain boundaries and arrive at the Ta/TaN interface. Since the TaN layer is not fully crystallized, these Cu atoms would have to find TaN grain boundaries or some local defects to diffuse to the Si substrate. This suggests that Cu atoms have to diffuse through a longer path to reach the Si substrate for the Ta/TaN bi-layer than a single Ta or TaN layer. It is equivalent to increase the effective thickness of the diffusion barrier. Thus, although TaN crystallization was detected by XRD and TEM, it still needed higher annealing temperature to active the Cu diffusion through Ta/TaN bi-layer barriers and react with Si substrate.

The microstructure evolution for the Cu/Ta/TaN bi-layer structure on the Si or SiO_2 during annealing can be described as follows according to the results above. With the increasing annealing temperature, N in the original TaN layer would diffuse to the neighboring Ta layer and caused the mixing of the Ta and TaN layer. And Ta would diffuse out to the Cu surface, reducing the total barrier thickness. Also at high annealing temperature, a $CuTa_{10}O_{26}$ ternary oxide formed which would increase the sheet resistance of the sample. The mixing of the Ta and TaN layer to one TaN layer would make easier crystallization of the TaN layer. The polycrystalline TaN grain boundaries provided fast diffusion path for Cu and caused failure of the barrier finally.

From the above discussion, we can expect how to reduce the barrier thickness in the future 65 nm technology node and beyond if we still use the Ta-based barrier. We should still use a bi-layer structure with thin TaN thickness and a slightly thicker Ta thickness. According to the discussion above, thin TaN layer would have a high crystallization temperature. Since Ta would outdiffuse to the Cu surface and cause the thinning of the barrier, a thicker Ta layer would be needed. Our research results have demonstrated (not shown here) that the Cu(50 nm)/Ta(5 nm)/TaN(3 nm)/Si structure has much better thermal stability than the Cu(50 nm)/TaN(8 nm)/Si structure.

5. Conclusion

Three diffusion barriers including Ta, TaN and Ta/TaN have been compared. The Ta/TaN bi-layer structure shows superior diffusion barrier properties for copper, without Cu_3Si formation until annealing at 950 °C. The advantages for the bi-layer structure over single Ta or TaN barrier were investigated. It reveals that the TaN crystallization temperature is film thickness-dependent, i.e. thinner TaN film has higher crystallization temperature. The better thermal stability for bi-layer structure is attributed to a good balance of the total barriers thickness and polycrystalline TaN crystallization temperature. The bi-layer structure provides thick enough barrier with additional Ta layer while the TaN layer itself is still thin to have high crystallization temperature. Grain boundaries mismatch between Ta and TaN also increases the difficulty for Cu diffusion through bi-layer structure. The microstructure evolution for Cu/Ta/TaN on the either Si or SiO_2 substrate is studied. It is expected that the future barrier structure in the 65 nm technology node or beyond should still use a Ta/TaN bi-layer with a thin TaN layer and a slightly thicker Ta layer.

Acknowledgements

This work was supported by National Natural Science Foundation in China (NSFC-60476010), Science and Technology Committee of Shanghai Municipality (04QMX1407) and the Bilateral Scientific and Technological Cooperation Project Flanders-China (B/06086/01). The authors would like to thank Novellus Systems Inc. for the donation of Cu technology toolsets and Dr. Chien Chiang's continuous support.

References

[1] K. Holloway, P.M. Fryer, C. Cabral Jr., J.M.E. Harper, P.J. Bailey, K.H. Kelleher, J. Appl. Phys. 71 (1992) 5433.
[2] T. Laurila, K. Zeng, J.K. Kivilahti, J. Appl. Phys. 88 (2000) 3377.
[3] L. Liu, Y. Wang, H. Gong, J. Appl. Phys. 90 (2001) 416.
[4] K.W. Kwon, C. Ryu, R. Sinclair, S. Simon Wong, Appl. Phys. Lett. 71 (1997) 3069.
[5] K.W. Kwon, H.J. Lee, R. Sinclair, Appl. Phys. Lett. 75 (1999) 935.
[6] M.H. Tsai, S.C. Sun, C.E. Tsai, S.H. Chuang, H.T. Chiu, J. Appl. Phys. 79 (1996) 6932.
[7] W.-H. Lee, J.-C. Lin, C. Lee, Mater. Chem. Phys. 68 (2001) 266.
[8] J.H. Wang, L.J. Chen, Z.C. Lu, C.S. Hsiung, W.Y. Hsieh, T.R. Yew, J. Vac. Sci. Technol. B 20 (2002) 1522.
[9] K.-L. Ou, W.-F. Wu, C.-P. Chou, S.-Y. Chiou, C.-C. Wu, J. Vac. Sci. Technol. B 20 (2002) 2154.
[10] Z.L. Yuan, D.H. Zhang, C.Y. Li, K. Prasad, C.M. Tan, Thin Solid Films 462/463 (2004) 284.
[11] M. Hecker, D. Fischer, V. Hoffmann, H.-J. Engelmann, A. Voss, N. Mattern, C. Wenzel, C. Vogt, E. Zschech, Thin Solid Films 414 (2002) 184.
[12] S. Tsukimoto, M. Moriyama, M. Murakami, Thin Solid Films 460 (2004) 222.

[13] S.S. Wong, C. Ryu, H. Lee, A.L.S. Loke, K.-W. Kwon, B.S.R. Eaton, R. Faust, B. Mikkola, J. Mucha, J. Ormando, in: Proceedings of the International Interconnect Technical Conference, IEEE, 1998, p. 107.
[14] M. Stavrev, D. Fischer, F. Praessler, C. Wenzel, K. Drescher, J. Vac. Sci. Technol. A 17 (1999) 993.
[15] H. Wang, A. Tiwari, A. Kvit, X. Zhang, J. Narayan, Appl. Phys. Lett. 80 (2002) 2323.
[16] G.S. Chen, S.C. Huang, S.T. Chen, T.J. Yang, Appl. Phys. Lett. 76 (2000) 2895.
[17] R. Hubner, M. Hecker, N. Mattern, V. Hoffmann, K. Wetzig, Ch. Wenger, H.-J. Engelmann, Ch. Wenzel, E. Zschech, J.W. Bartha, Thin Solid Films 437 (2003) 248.
[18] L.Y. Yang, D.H. Zhang, C.Y. Li, P.D. Foo, Thin Solid Films 462/463 (2004) 176.
[19] R. Hubner, M. Hecker, N. Mattern, V. Hoffmann, K. Wetzig, Ch. Wenger, H.-J. Engelmann, Ch. Wenzel, E. Zschech, Thin Solid Films 458 (2004) 237.
[20] G.S. Chen, P.Y. Lee, S.T. Chen, Thin Solid Films 353 (1999) 264.
[21] S.M. Rossnagel, J. Vac. Sci. Technol. B 20 (6) (2002) 2328.
[22] K.M. Yin, L. Chang, F.R. Chen, J.J. Kai, C.C. Chiang, G. Chuang, P. Ding, B. Chin, H. Zhang, F. Chen, Thin Solid Films 388 (2001) 27.
[23] C. Gu, P.W. Lynch, A.B. Yang, C.G. Olson, Phys. Rev. B 42 (1990) 1526.
[24] F.M. d'Heurle, J. Mater. Res. 3 (1988) 167.
[25] C. Detavernier, R.L. Van Meirhaeghe, F. Cardon, Phys. Rev. B 62 (2000) 12045.
[26] Z. Ma, L.H. Allen, Phys. Rev. B 49 (1994) 13501.
[27] Z. Ma, L.H. Allen, D.D.J. Allman, Thin Solid Films 253 (1994) 451.